Journal of Nuclear Materials 196–198 (1992) 194–198
North-Holland

journal of nuclear materials

Effect of boundary conditions on the neutral gas temperatures and densities in the ITER divertor and pump duct

D.N. Ruzic and D.R. Juliano
University of Illinois, 103 South Goodwin Avenue, Urbana, IL 61801, USA

The DEGAS neutral atom transport code was used to simulate helium pumping and D/T throughput in ITER. The sensitivity of the simulation to two different reflection models, four transmission probabilities from the exit of the simulation to the pump (0.0625, 0.125, 0.1875 and 0.250), and a 2-D model versus a 3-D model were analyzed. The variation in reflection model changes the densities in the duct and the recycling of D/T by a factor of 1.6. The variation in the transmission probabilities affects these same quantities by a factor of 2.5. The dimensionality of the simulation affects the density profile in the duct. A transmission probability from the exit of the DEGAS simulation to the pump of 0.110 to 0.125 was calculated from the ITER reference drawings. Using this quantity and the DEGAS results, an exhaust rate of 112 to 127 moles/h is predicted, implying that the reference pumping systems may be larger than necessary by a factor of 2.

1. Introduction

This work examines the effects of neutral atom reflection, pump duct albedo and code dimensionality on the simulation of the He and D/T exhaust performance of the International Thermonuclear Experimental Reactor (ITER). These boundary conditions affect the neutral atom recycling and throughput calculations by a factor of 2–3. Knowledge of the expected densities, and the ability to increase them while maintaining the same plasma edge conditions could reduce the size of the pumping system and its access requirements by a similar magnitude.

This work couples the DEGAS [1] and B2 [2] codes. B2 is a 2-D fluid transport code which solves the coupled continuity, momentum balance and energy balance equations. DEGAS is a 3-D Monte Carlo neutral species transport code rich in atomic physics. The B2 and DEGAS codes were iterated until their respective boundary conditions at the divertor plate matched. The iteration procedure, B2 input conditions for the ITER physics phase double-null ignited plasma, and the resultant edge plasma parameters and divertor plate flux profiles, have been described previously [3]. Those identical plasma conditions were used for all the work in this paper. The current of helium to the divertor plate is taken at 0.1 of the D/T current.

Fig. 1 shows the 2-D geometry used in most of these calculations. This geometry differs from the ITER reference geometry by the elongation of the divertor "nose". Previous work [3] showed this "big nose" geometry to exhaust He preferentially to D/T by a factor of 2.01 ± 0.54 compared to the reference geometry. The lower X-point and outboard divertor strike point are shown. The right hand boundary of the figure is the opening to the pump duct. The albedo of that exit plane was adjustable to match the conductance and pumping speed of the rest of the pumping system.

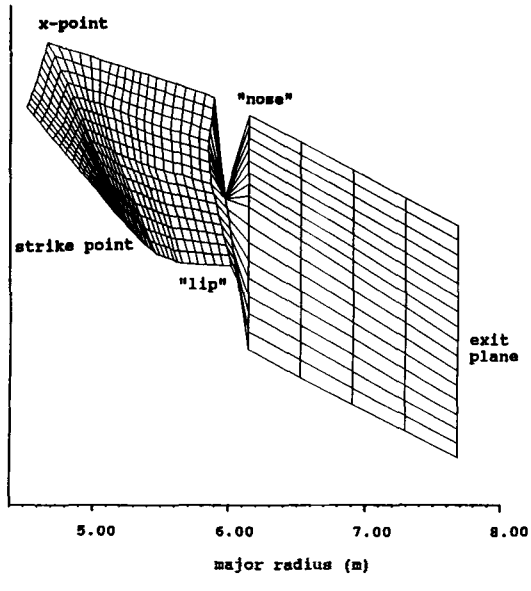

Fig. 1. Two-dimensional grid used for the DEGAS simulations of ITER.

Each of the 16 segments along that wall could be treated as exits or mirrors. The boundaries with the plasma were all treated as mirrors for neutral atoms, but few if any particles remained unionized to reach those boundaries. The other walls were simulated as carbon.

The next section describes the effects of two differing wall reflection models. This is followed by an analysis of pump duct albedo and the variation from 1 to 4 of the wall segments acting as exits. Finally a 3-D simulation is compared to the 2-D simulations to show the effect of nontoroidal symmetry in the pump ducts.

2. Reflection

Fig. 2a shows the number reflection coefficients, R_n, for normally incident D and He on C as a function of energy. The data showing reflection becoming 0 at 0 eV is from VFTRIM (vectorized fractal TRIM) [4,5] simulations using a fractal dimension of 2.10. The other graphs showing no variation from 0 to 10 eV are from the standard DEGAS reflection data file used in the USA until March 1992. This standard data is similar to that described in ref. [6] for normal incident particles. Fig. 2b shows the associated energy reflection coefficient, R_e, for D and He on C for the two cases. VFTRIM simulates atomic scale surface topography with a fractal model and compares well with experiments. It predicts fewer and less energetic atomic reflections for D than the standard DEGAS package while predicting more direct He reflections. The models treat reflection at higher angle of incidence in different manners as well. Both models use a cosine distribution for the direction of the reflecting flux, but the values of R_n were simply doubled if the incident angle, θ, was greater than 40° from normal in the standard DEGAS model. The new VFTRIM model sets

$$R_n(\theta) = R_n(0)(1 + 0.5 \sin \theta). \quad (1)$$

In both cases the maximum R_n allowed is 0.9.

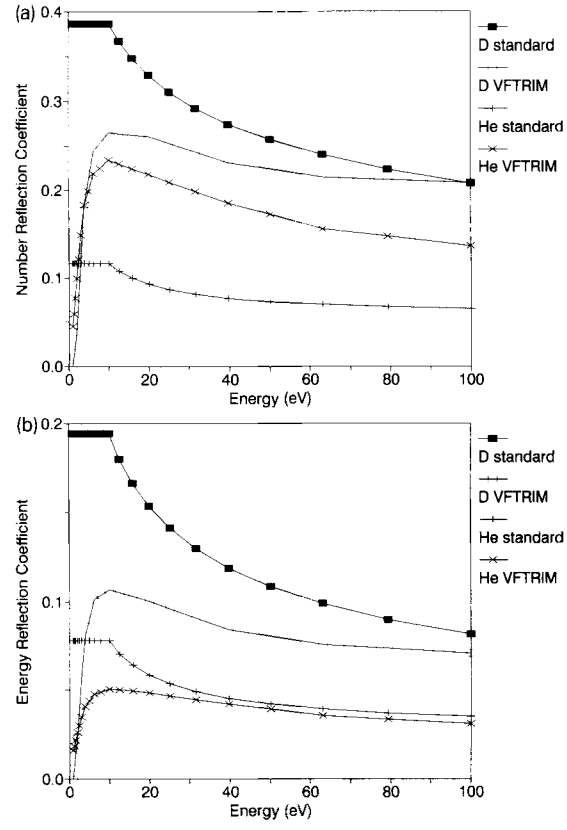

Fig. 2. Reflection coefficients used in the VFTRIM reflection model and the standard DEGAS reflection model for D and He on C at normal incidence as a function of energy: (a) number of atoms reflected per incident particle; (b) fraction of energy retained for those particles which reflect.

The effect of these different wall models on the neutral densities and recycling is summarized in table 1. The density of D/T atoms is indeed reduced utilizing the new reflection data. Atoms are turned into thermal molecules more quickly thus leading to a higher average number of wall collisions per flight. Conversely, the energetic helium is preserved longer with the new reflection model. This leads to a lower density

Table 1
Effects of the change of surface reflection model on the neutral atoms and molecules in the pump duct. The standard error in the atomic D/T density is roughly 30%. The standard error in the molecular $(D/T)_2$ density is roughly 15%. The standard error in the He density is roughly 10%

	Density (10^{19} m^{-3})			$R_{D/T}$	R_{He}	Average wall collisions per flight initiated by	
	D/T	$(D/T)_2$	He			D/T	He
VFTRIM	0.028	3.29	1.44	0.947 ± 0.007	0.909 ± 0.009	5.44	9.13
Standard	0.084	2.30	1.70	0.968 ± 0.005	$0.910 + 0.009$	4.83	10.3

and fewer wall collisions per flight on average. The DEGAS data presented in ref. [3] also used reflection data from an earlier version of VFTRIM.

The effects on the He and $(D/T)_2$ recycling and throughput are more complicated: No particles are absorbed by the walls. Therefore a particle is either ionized by the plasma or passes through an exit to the pumps. The recycling coefficient, R, is a measure of that branching ratio. If 1000 particles strike the divertor plate and 53 pass through the exit aperture, $R = 1 - (53/1000) = 0.947$. The VFTRIM model reduced $R_{D/T}$ leaving R_{He} unchanged. Recycling is dependent on the reflection conditions, but closely connected with geometrical considerations.

The reflection model effects on recycling and the utility of the "big nose" geometry can be seen by comparing the neutral D/T atom temperatures and densities as a function of position for the two reflection models. The "nose" prevents energetic neutral atoms from returning to the plasma. Higher temperatures and densities of neutral D/T atoms trapped on the duct side are some of the nose features. Using the standard DEGAS reflection model, little temperature and density variation within the duct is seen. In the standard model the initial high incident angle reflection from the divertor plate sends many more atoms deep into the pump duct where they bounce from the top and bottom walls. Since reflection is always taken with a cosine distribution from the wall normal, not specular reflection, these atoms or molecules have as large of a chance of returning to the plasma as they do of exiting the simulation.

With the VFTRIM model's lower R_n and R_e there are fewer fast atoms injected into the duct, but the ones that do enter the duct with significant energies are primarily those born on the divertor plate lip. The neutral atom temperature and atomic density are higher near the divertor plate lip. Once these atoms reflect near the opening they will preferentially strike the upper duct boundary just inside the nose. At this point they cannot return directly to the plasma. There are more direct reflections from the duct side of the nose whose surface normal points toward the duct opening thus leading to a more directed flux down the pipe and hence a lower recycling rate. The atomic densities and thus the molecular source rates are higher along the top of the duct and just inside the nose.

3. Albedo

Not all of the particles striking the simulation space exit plane will be removed by the pumps. A molecular transmission probability, a, must be calculated for the specific ITER pumping geometry and pumping system. The number of "exits" in the DEGAS simulation is then matched to this transmission probability. If $a = 0.125$ then two of the 16 cell boundaries would allow particles to leave the simulation and the other 14 would reflect the particles as a mirror.

The actual ITER pump duct geometry extends approximately 12 m beyond and 4 m below the exit plane of the simulation space making two gentle 45° bends in opposite directions and obtaining a circular cross section of 2.0 m diameter [7]. There are 16 such ducts equally spaced around the torus with an estimated 150 m^3/s pumping speed on each duct.

Treating the duct as a 2 m diameter diagonal pipe, 13.2 m long and following the Monte Carlo conductance calculation techniques presented in ref. [8], the molecular transmission probability of the pipe, a_p, is 0.27. If instead the duct is treated as a 12 m and a 4 m section connected by a right angle bend, $a_p = 0.20$. Therefore the conductance, C, of one 2 m diameter pipe for 300 K $(D/T)_2$ with an average velocity, $v = 1144$ m/s is 242 to 180 m^3/s for the two different

Table 2
Effect of the simulation exit plane albedo on the neutral atoms and molecules in the pump duct for coincident D/T and He ion flux profiles and for an outward 20 cm shift of the He profile with respect to the D/T profile. The standard error in the atomic D/T density is roughly 30%. The standard error in the molecular $(D/T)_2$ density is roughly 15%. The standard error in the He density is roughly 10%

Exit plane openings	Density (10^{19} m^{-3})				Recycling		
	D/T	$(D/T)_2$	He	He shifted	$R_{D/T}$	R_{He}	R_{He} shifted
1/16	0.029	4.16	1.87	3.96	0.977 ± 0.005	0.948 ± 0.007	0.896 ± 0.010
2/16	0.027	3.29	1.44	2.70	0.947 ± 0.007	0.911 ± 0.009	0.826 ± 0.013
3/16	0.024	3.08	1.36	2.45	0.954 ± 0.007	0.890 ± 0.010	0.797 ± 0.014
4/16	0.022	1.66	0.89	1.76	0.947 ± 0.007	0.872 ± 0.011	0.783 ± 0.015

values of a_p. For 16 ducts and a total pumping speed of 2400 m^3/s, the effective pumping speed at the exit of the DEGAS simulation space, S_D, is 1483 to 1308 m^3/s. The appropriate molecular transmission probability for the DEGAS simulation, a_D, can now be found from:

$$S_D = (\text{average velocity}/4)(\text{area})a_D. \quad (2)$$

For $S_D = 1483$ to 1308 m^3/s, $v = 1144$ m/s and area equal to $(1.6 \times 2.0 \times 16)$ m^2, $a_D = 0.125$ to 0.110. Accordingly, an a_D of 0.125 was used for all the calculations in section 2 as well as those in ref. [3].

A helium density of 1.44×10^{19} m^{-3} at the DEGAS exit plane and a pumping speed at that plane of 1483 to 1308 m^3/s exhausts 127 to 112 moles/h. This significantly exceeds the design specification [7] fueling and exhaust rate of 35 to 75 moles/h, implying that the reference pumping systems may be larger than necessary.

Table 2 shows the effects of varying a_D from $\frac{1}{16}$ to $\frac{4}{16}$ on the densities and recycling coefficients. As expected the densities drop as the transmission probability increases. The effect on recycling He follows a similar trend. More particles exit as the number of exits is increased. On the other hand, the D/T exiting current levels off as the number of exits is increased. This can be explained by looking at the average energy of the exiting flux. The D/T molecules are all at thermal energies while the He atoms have an average exit energy of 0.6 to 0.8 eV. Of the D/T nuclei that exit approximately 10% exit as atoms with an average energy of 2.0 to 3.0 eV. Energetic atoms retain a larger measure of directed flux than thermal molecules. Even at $a_d = 0.25$ the opening to the plasma is larger than the opening in the duct.

Also shown in table 2 are results from shifting the helium flux profile on the divertor plate 20 cm outward (away from the separatrix) with respect to the D/T flux profile. This simulates the possible effect of drifts or minority species edge heating. The helium densities once again drop significantly and still more exit as the opening is increased. The average exit energy is lowered to 0.5–0.6 eV.

4. Nontoroidal symmetry

In a 2-D DEGAS simulation the third (toroidal) direction is tracked. However, there are no boundaries in this direction. It is as if the particles were travelling between parallel plates, the top and bottoms of the duct. In a full 3-D simulation there will be collisions with the sides of the duct. To isolate this effect a rectangular duct 140 cm by 140 cm and 700 cm long was simulated with the DEGAS code. This duct was connected to a slanted divertor plate containing the same B2/DEGAS-iterated plasma. A 2-D simulation using the same plasma and geometry was run for a comparison.

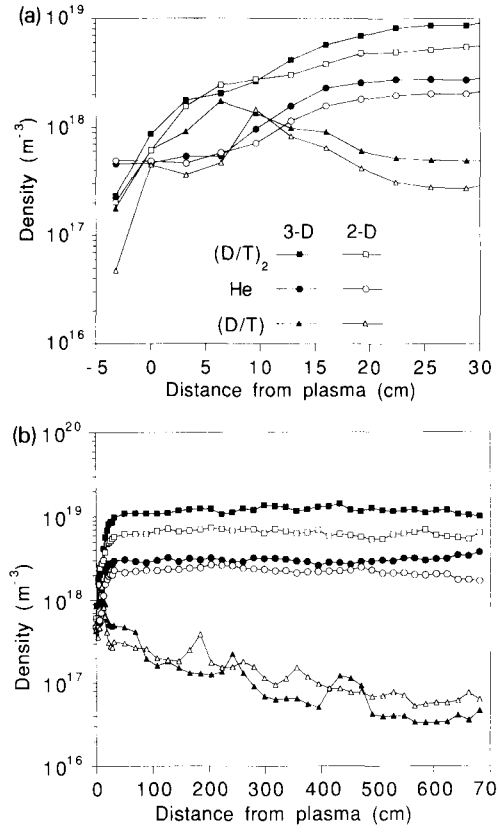

Fig. 3. Comparison of 2-D and 3-D simulations of a rectangular duct with the ITER divertor plate and plasma at one end and a exit plane albedo of 0.125 at the other end. The same ion current density on the plate was used for each case. The bumps on the 2-D and 3-D $(D/T)^0$ curves between 100 and 700 cm are indicative of the magnitude of the Monte Carlo noise.

Fig. 3 shows the atomic and molecular densities as a function of distance from the plasma. Near the plasma boundary (−5 to 5 cm) the He and $(D/T)_2$ densities do not significantly vary. The effect of increased wall collisions is most evident when comparing the D/T atomic density profiles. The peak of the neutral atom density occurs closer to the plasma for the 3-D case because the increased number of wall collisions makes it more difficult for the atoms to be transmitted down the pipe. Flights initiated by D/T^+ and He^{2+}, respectively, suffer 6.0 and 9.2 wall collisions on average for the 2-D simulation and 16.2 and 22.5 wall collisions on average for the 3-D simulation. This larger number of wall collisions for the 3-D case also leads to a smaller

throughput and hence a higher ultimate density in the duct for the 3-D simulation.

5. Summary and future work

An accurate wall reflection model and consistent duct albedo estimates are essential for detailed calculations of pump duct densities and recycling. Recycling and gas throughput depend significantly on the boundary conditions and geometry of the simulation. These calculations indicate that the reference pumping systems for ITER may be larger than necessary by approximately a factor of 2.

Other effects should also be included in the pumping calculations. The present simulation ignores neutral–neutral collisions which may be significant in the ITER geometry. In addition the exit plane "mirrors" should reflect atoms as thermal molecules to better simulate the back conductance of the pumping system. Ideally a differing albedo for He and D/T should exist due to their differing pumping speeds. These refinements will be included in future work.

Acknowledgements

This work was performed under DOE contract no. DOE-DEFG-02-89-ER52159.

References

[1] D.B. Heifetz et al., J. Comput. Phys. 46 (1982) 309.
[2] B. Braams, Eur. Conf. on Controlled Fusion and Plasma Physics, Part II, Budapest, 1985, p. 480.
[3] D.N. Ruzic, K.A. Werley and S.A. Cohen, J. Nucl. Mater. 176 & 177 (1990) 926.
[4] D.N. Ruzic, Nucl. Instr. and Meth. B47 (1990) 118.
[5] M. Shaheen and D.N. Ruzic, submitted to Model. Simul. Mater. Sci. Eng.
[6] W. Eckstein and D.B. Heifetz, J. Nucl. Mater. 145–147 (1987) 332.
[7] ITER Conceptual Design Activity Document and ITER engineering drawing no. 3711/1-1.
[8] J.F. O'Hanlon, A User's Guide to Vacuum Technology, 2nd ed. (Wiley, New York, 1989) pp. 36–48.